Quasi-elastic neutrino charged-current scattering of medium-heavy nuclei: ^{40}Ca and ^{40}Ar

A. Butkevich

Institute for Nuclear Research, Moscow

20 December 2011

Femilab, PPD/Neutrino Physics Discussion

Motivation

- ($\star$) To make neutrino detectors fully active, highly segmented and fine-grained scintillator (^{12}C) is used as target and detecting material.
- ($\star$) Liquid Argon TPC are one of the most perspective technologies for next generation of neutrino detector ICARUS, MickroBooNe, LNBE.
- ($\star$) There are no the cross section data about quasi-elastic electron and neutrino scattering off Argon. On the other hand there are precision data for electron scattering on ^{40}Ca target. The structures of ^{40}Ca and ^{40}Ar are almost identical.
- ($\star$) Therefore it is reasonable to calculate cross sections of QE electron scattering off ^{40}Ca target to test models predictions against e^{40}Ca data.
- ($\star$) In long baseline neutrino experiments the near and far detectors are not necessary of the same target material. It is important to compare the CCQE cross sections for neutrino scattering off ^{12}C, ^{16}O, and ^{40}Ar targets.

Formalism of the CCQE Scattering

Lepton CC QE exclusive reaction

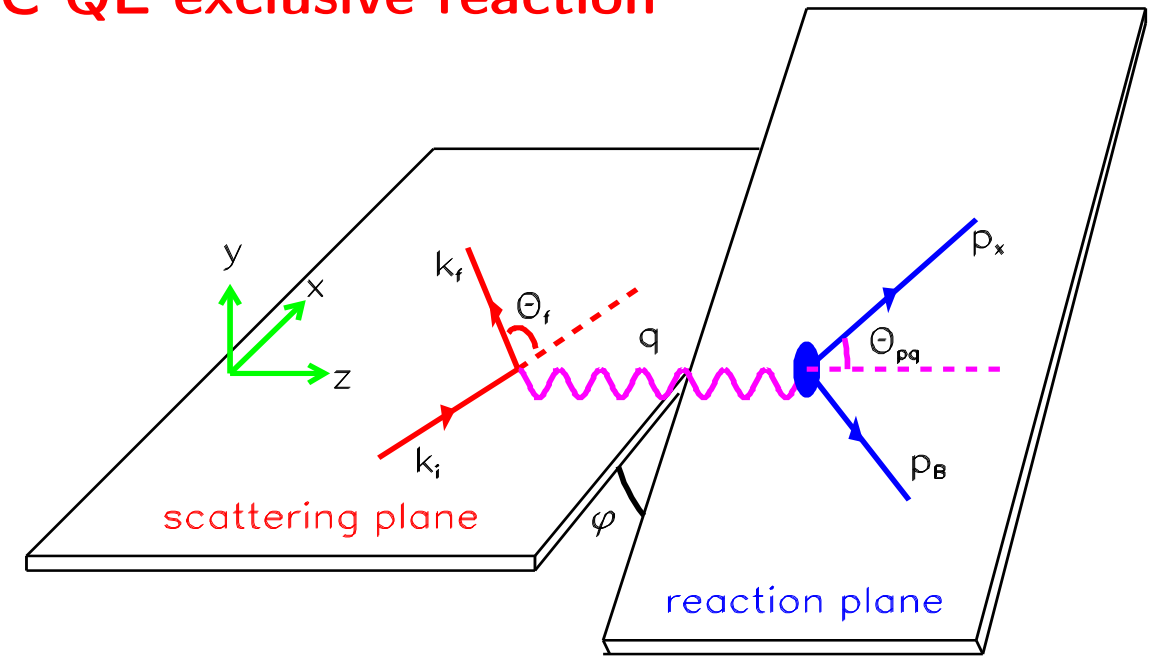

$$l(k_i) + A(p_A) \rightarrow l'(k_f) + N(p_x) + B(p_B),$$

$$\frac{d^5\sigma^{el}}{d\varepsilon_f d\Omega_f d\Omega_x} = R\frac{|\mathbf{p}_x|\varepsilon_x}{(2\pi)^3}\frac{\varepsilon_f}{\varepsilon_i}\frac{\alpha^2}{Q^4}L^{(el)}_{\mu\nu}W^{\mu\nu(el)}$$

$$\frac{d^5\sigma^{cc}}{d\varepsilon_f d\Omega_f d\Omega_x} = R\frac{|\mathbf{p}_x|\varepsilon_x}{(2\pi)^5}\frac{|\mathbf{k}_f|}{\varepsilon_i}\frac{G^2\cos^2\theta_c}{2}L^{(cc)}_{\mu\nu}W^{\mu\nu(cc)},$$

$L_{\mu\nu}$ and $W^{\mu\nu}$ are lepton and hadronic tensors. ε_f, Ω_f are energy and solid angle of the scattered lepton. Ω_x is solid angle for ejectile nucleon momentum.

Formalism

The weak CC hadronic tensor $W_{\mu\nu}$ is given by bilinear product of the transition matrix elements of the nuclear CC operator J_μ between the initial nucleus state $|A\rangle$ and the final state $|B_f, \mathrm{p}_x\rangle$ as

$$W_{\mu\nu} = \sum \langle B_f, p_x | J_\mu | A \rangle \langle A | J_\nu | B_f, p_x \rangle$$

It is also useful to define a **reduced cross section**

$$\sigma_{red} = \frac{d^5\sigma}{d\varepsilon_f d\Omega_f d\Omega_x} / K\sigma_{lN},$$

where K is phase-space factor for lepton scattering, and σ_{lN} is corresponding elementary cross section for the lepton scattering from moving free nucleon. σ_{red} should be similar for electron and neutrino scattering (apart from small differences due to coulomb corrections and FSI effects for electron and neutrino induced reactions).

In the **inclusive reactions** only the outgoing lepton is detected and the differential cross sections can be written as

$$\frac{d^3\sigma^{el}}{d\varepsilon_f d\Omega_f} = \frac{\varepsilon_f}{\varepsilon_i} \frac{\alpha^2}{Q^4} L^{(el)}_{\mu\nu} \mathcal{W}^{\mu\nu(el)},$$

$$\frac{d^3\sigma^{cc}}{d\varepsilon_f d\Omega_f} = \frac{1}{(2\pi)^2} \frac{|\mathrm{k}_f|}{\varepsilon_i} \frac{G^2 \cos^2\theta_c}{2} L^{(cc)}_{\mu\nu} \mathcal{W}^{\mu\nu(cc)}$$

where $\mathcal{W}^{\mu\nu}$ is inclusive hadronic tensor.

Nuclear matrix element

- We describe the lepton-nucleon scattering in the Impulse Approximation (IA), in which only one nucleon of the target is involved in reaction and the nuclear current is written as the sum of single-nucleon currents.

$$\langle p, B|J^{\mu}|A\rangle \quad = \quad \sum \int d^3r \ \exp(it \cdot r)\overline{\Psi}^{(-)}(p, r)\Gamma^{\mu}\Phi(r),$$

where Γ^{μ} is the vertex function, Φ and $\Psi^{(-)}$ are relativistic bound-state and outgoing wave functions.

- Electromagnetic current vertex in CC2 scheme

$$\Gamma^{\mu}_{V} = F_V(Q^2)\gamma^{\mu} + i\sigma^{\mu\nu}q_{\nu}F_M(Q^2)/2m \qquad (2)$$

- The single-nucleon charged current has $V-A$ structure $J^{\mu} = J^{\mu}_{V} + J^{\mu}_{A}$ and for $\Gamma^{\mu} = \Gamma^{\mu}_{V} + \Gamma^{\mu}_{A}$ we use a free nucleon vertex function

$$\Gamma^{\mu}_{V} = F_V(Q^2)\gamma^{\mu} + i\sigma^{\mu\nu}q_{\nu}F_M(Q^2)/2m$$

and the axial current vertex function

$$\Gamma^{\mu}_{A} = F_A(Q^2)\gamma^{\mu}\gamma_5 + F_P(Q^2)q^{\mu}\gamma_5.$$

We use the MMD approximation [P.Mergell et al (1996)] of the vector nucleon form factors and the dipole approximation for the axial F_A and pseudoscalar F_P form factors.

Model

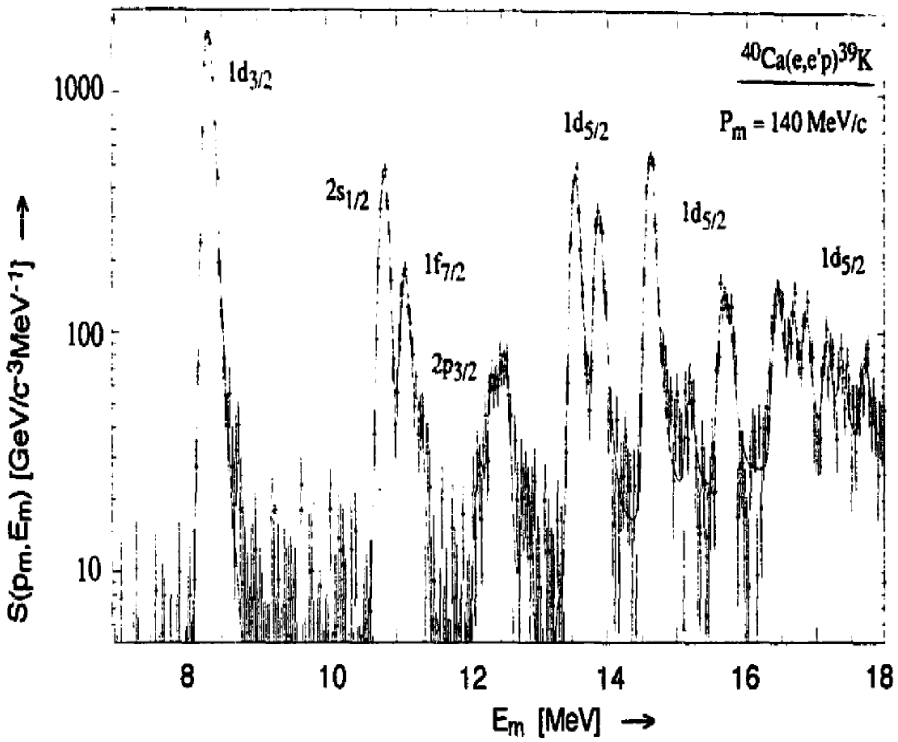

The typical excitation energy spectrum of ^{40}Ca measured in NIKHEF experiment in missing energy range $0 < \varepsilon_m < 23$ MeV. The knock-out from $1d_{3/2}, 2s_{1/2}, 1d_{5/2}, 1f_{7/2}$, and $2p_{3/2}$ are observed.

The σ_{red} cross sections in $^{40}Ca(e,e'p)^{39}K$ reaction were measured in the follow experiment:

Tokyo: K.Nakamura et al. Nucl.Phys.A271(1976)221, Saclay: M.Bernheim et al. Nucl.Phys. A375(1982)381, NIKHEF:G.J.Kramer et al. Phys.Lett. B227(1989)199, Nucl.Phys. A679(2001)267

In IPSM the model space for ^{40}Ca consists of 6 states for proton(neutron): $1d_{3/2}(4), 2s_{1/2}(2), 1d_{5/2}(6), 1p_{1/2}(2), 1p_{3/2}(4), 1s_{1/2}(2)$. The observed $1f_{7/2}$ and $2p_{1/2}$ is result of long-range nucleon correlations.

Model

Nucleon momentum distribution measured in Saclay experiment

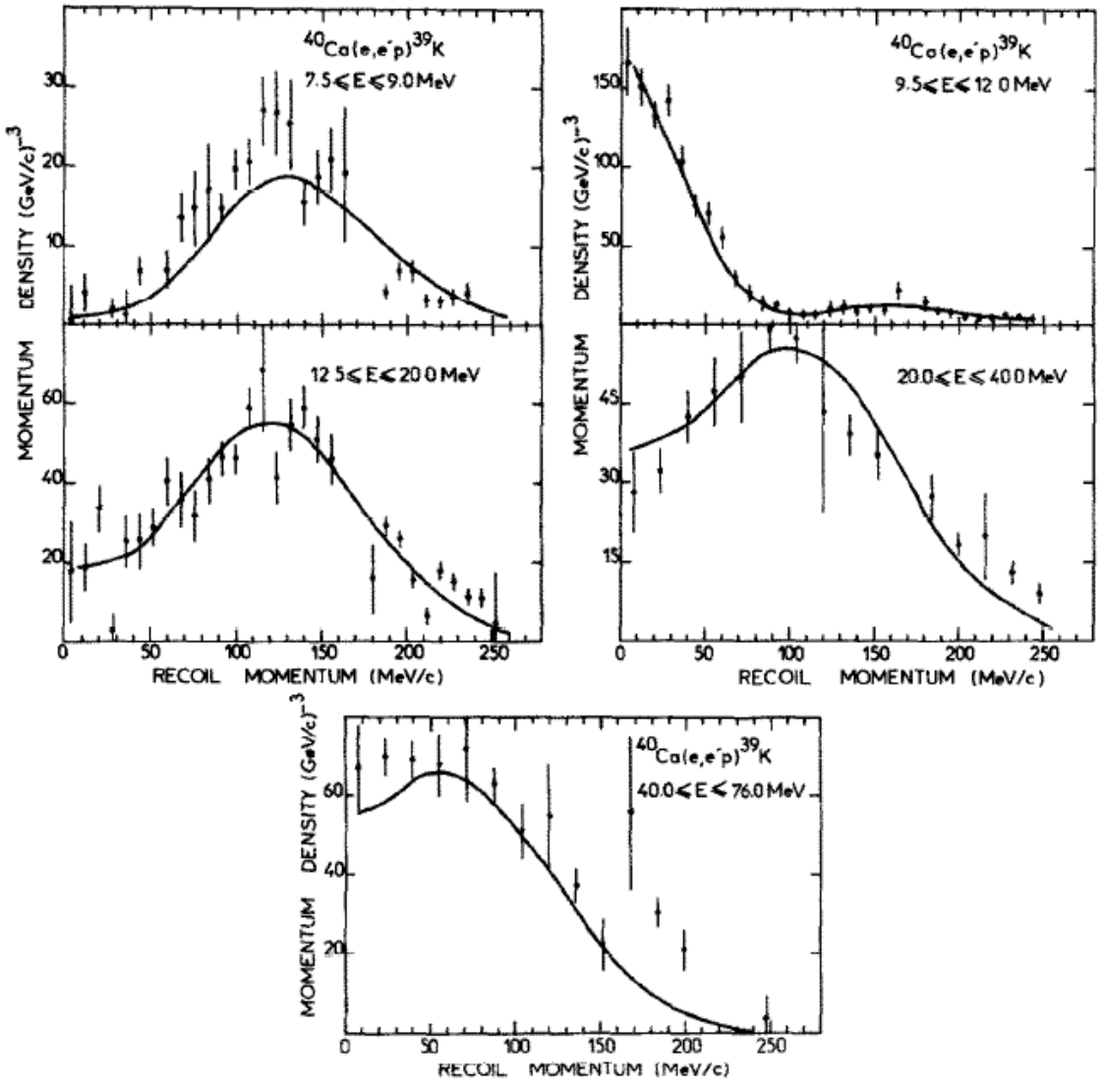

Fig. 14. Momentum distribution from ^{40}Ca(e, e′p); (a) $7.5 \leqq E \leqq 9$ MeV, (b) $9.5 \leqq E \leqq 12$ MeV, (c) $12.5 \leqq E \leqq 20$ MeV, (d) $20 \leqq E \leqq 40$ MeV and (e) $40 \leqq E \leqq 70$ MeV. The solid line represents the DWIA calculation.

Model

The value of the spectroscopic factors for ^{40}Ca orbitals were were deduced from $^{40}Ca(e,e'p)^{39}K$ reactions in *G.J.Kramer Ph.D. thesis (1991), G.J. Kramer et al. Phis.Lett. B227(1989)199, J.P.McDermott PRL65(1990)1991, C.Mahaux, R.Sator Nucl.Phys.A484 (1988)205, J.M. Udias et al. PRC48(1993)2731 and PRC51(1995)3246*.

The shape of momentum distribution is related to the shape of bound-state wave and the strength is proportional to the spectroscopic factors of the shells.

In this calculation we use the shell occupancy for ^{40}Ca
$S(1d_{3/2}) = 0.82, S(2s_{1/2}) = 0.845, S(1d_{5/2}) = 0.8, S(1p_{1/2}) = 0.95, S(1p_{3/2}) = 0.95, S(1s_{1/2}) = 1$,
for ^{40}Ar $S(1d_{3/2}) = 0.845, S(2s_{1/2}) = 0.845, S(1d_{5/2}) = 0.8, S(1p_{1/2}) = 0.95, S(1p_{3/2}) = 0.95, S(1s_{1/2}) = 1$ for proton and
$S(1f_{7/2}) = 0.82, S(1d_{3/2}) = 0.82, S(2s_{1/2}) = 0.85, S(1d_{5/2}) = 0.8, S(1p_{1/2}) = 0.95, S(1p_{3/2}) = 0.95, S(1s_{1/2}) = 1$ for neutron.

Average occupancy of nuclear shells $\bar{S} = 0.87$ and 13% of the missing strength can be attributed to the SRC(NN pair). Note that the calculation for the $1d_{3/2}$ and $2s_{1/2}$ states include the incoherent contributions of $1f_{7/2}$ and $2p_{1/2}$ states.

Shell occupancy for Oxygen:

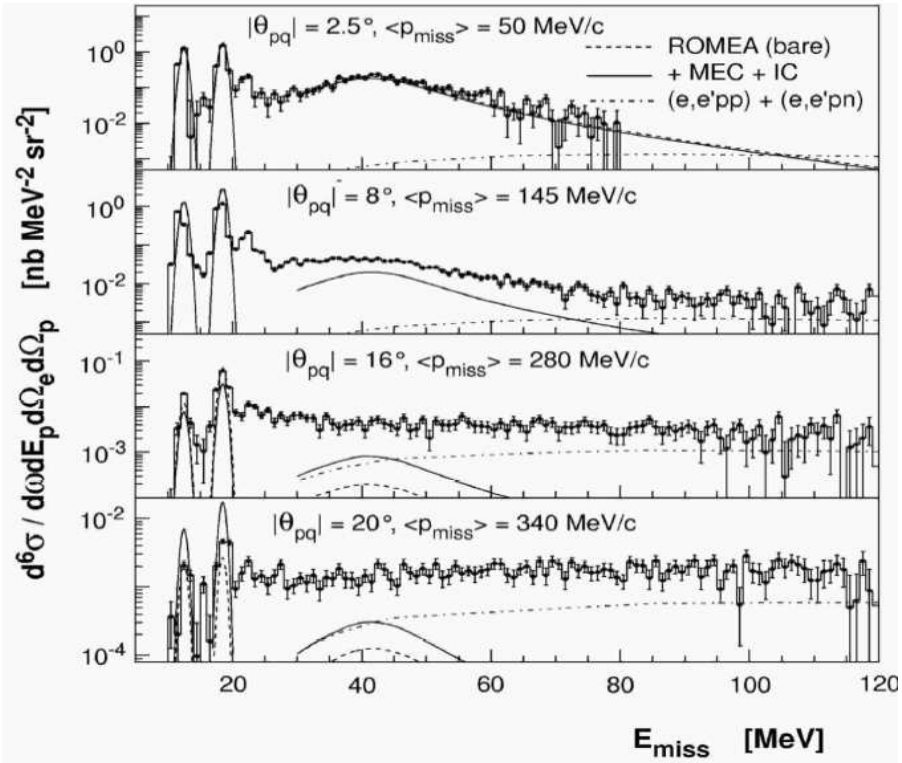

$S(P_{1/2})$=0.7

$S(P_{3/2})$=0.66

$S(S_{1/2})$=1

Average occupancy of nuclear shells $\overline{S}$=0.75

[supported by JLab measurement K. G. Fissum et al. (2005)]

Missing strength of 25% can be attributed to SRC

Shell occupancy for Carbon:

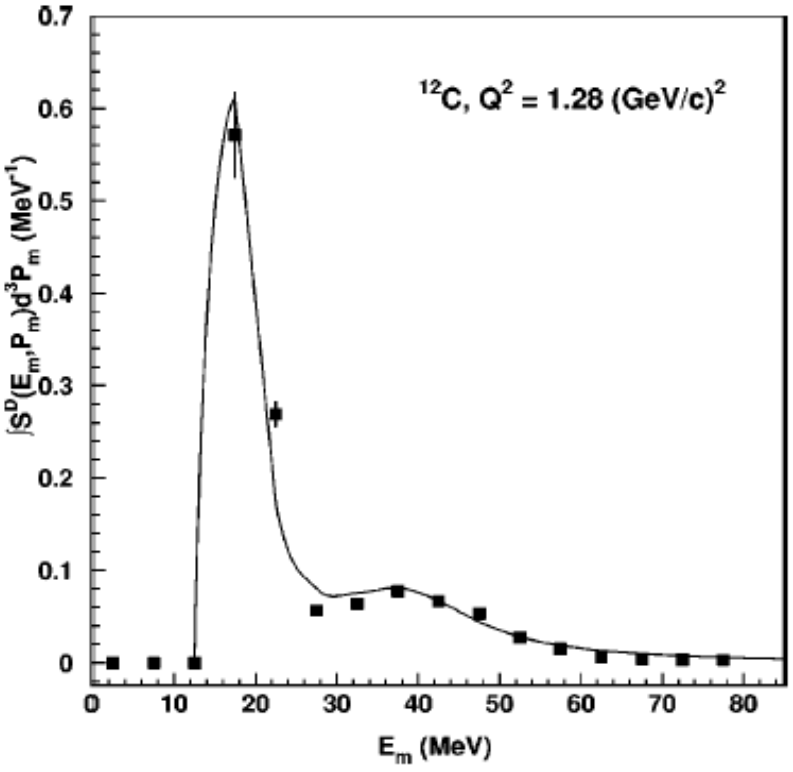

S($P_{3/2}$)=0.84

S($S_{1/2}$)=1

Average occupancy of nuclear shells $\overline{S}$=0.89

supported by JLab measurement [D. Dutta et al. (2003), J.J.Kelly (2004)]

Missing strength of 11% can be attributed to SRC.

JLab measurement [D.Rohe at al. (2006)] observed approximately 0.6 proton in a region with $p_m > 240$ MeV and $E_m > 50$ MeV.

Model

- In independent particle shell model the relativistic bound-state functions Φ are obtained within the Hartree–Bogolioubov approximation in the $\sigma - \omega$ model [B.Serot et al. 1986].
  - ⋆ In our calculations the spectral function P_{HM} incorporates 13% of the total normalization of the spectral function.
- In the RDWIA the final state interaction between the outgoing nucleon and the residual nucleus is taking into account and the ejectile wave function Ψ is a solution of a Schrödinger equation containing equivalent central and spin-orbit potentials, which are functions of the scalar and vector potentials S and V, and are energy dependent.
- In Fermi Gas model for Calcium and Argon we use p_F=249 MeV/c and ε=33 MeV. The RFGM does not account for nuclear shell structure, FSI effect, and the presence of NN-correlations.

RESULTS

Reduced cross sections

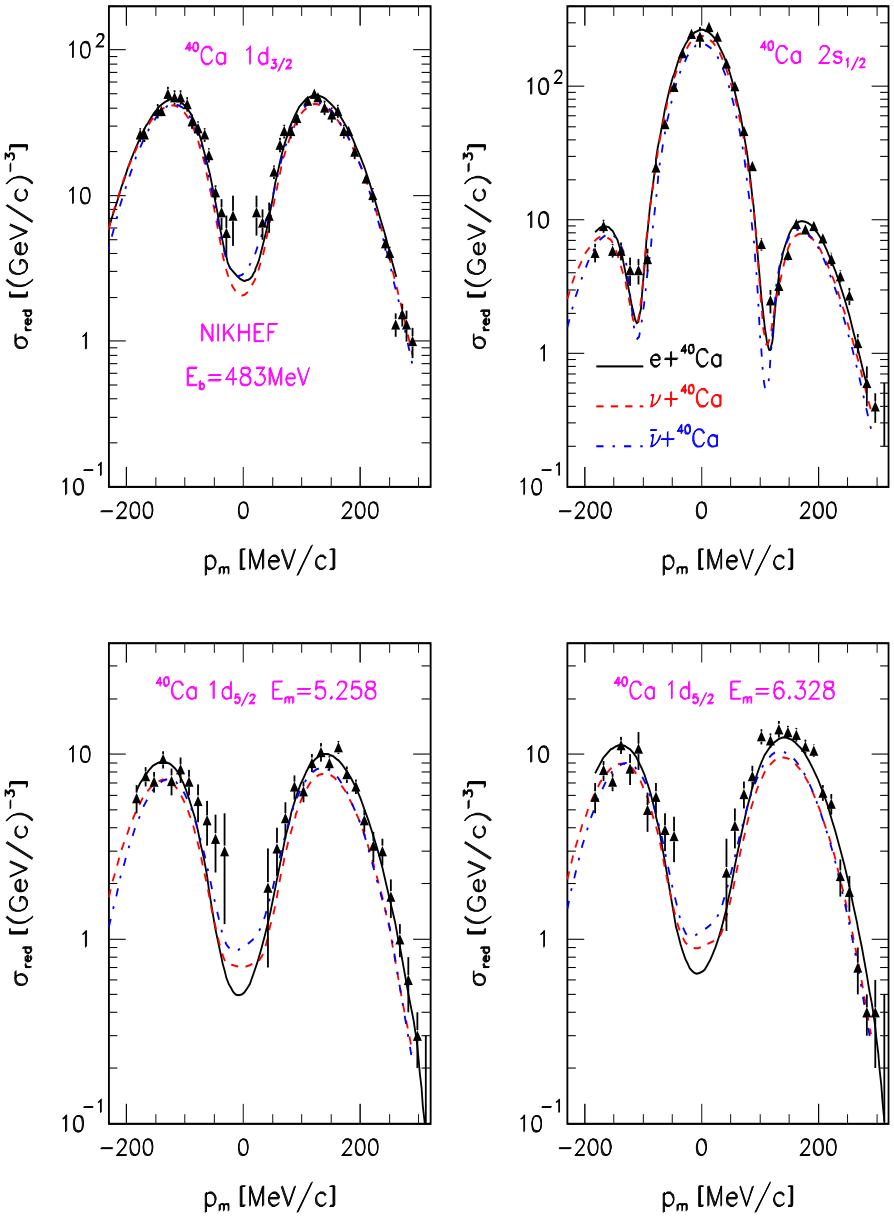

Comparison of the RDWIA calculations for electron, neutrino, and antineutrino reduced cross sections for the removal of nucleon from $\mathbf{1d_{3/2}}$, $\mathbf{2s_{1/2}}$ and $\mathbf{1d_{5/2}}$ shells of ^{40}Ca as a function of missing momentum. The cross sections were calculated for NIKHEF [G.J.Kramer (1991)] kinematics: $\boldsymbol{\varepsilon_i = 483}$ MeV, and $\boldsymbol{T_x = 100}$ MeV. Negative values of $\boldsymbol{p_m}$ correspond to $\boldsymbol{\phi = \pi}$ and positive ones to $\boldsymbol{\phi = 0}$.

Reduces cross sections

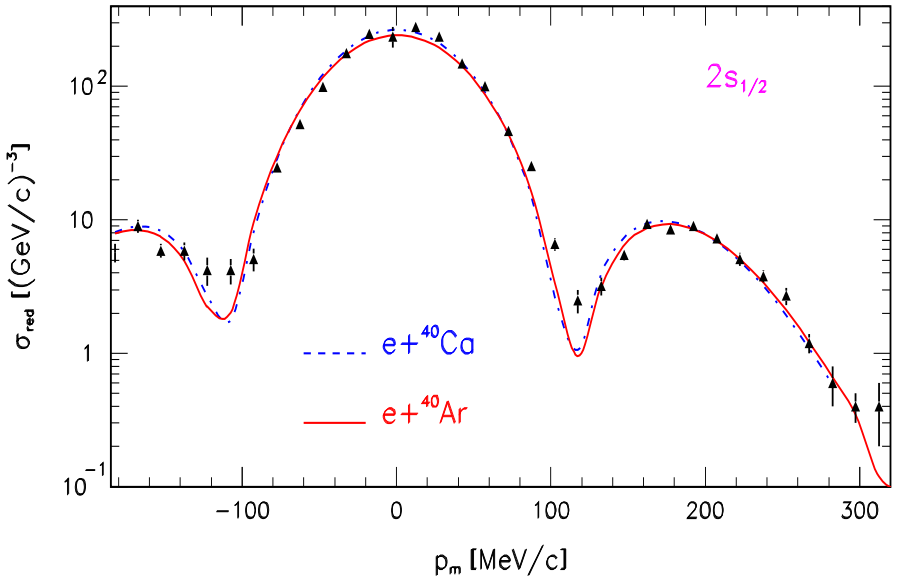

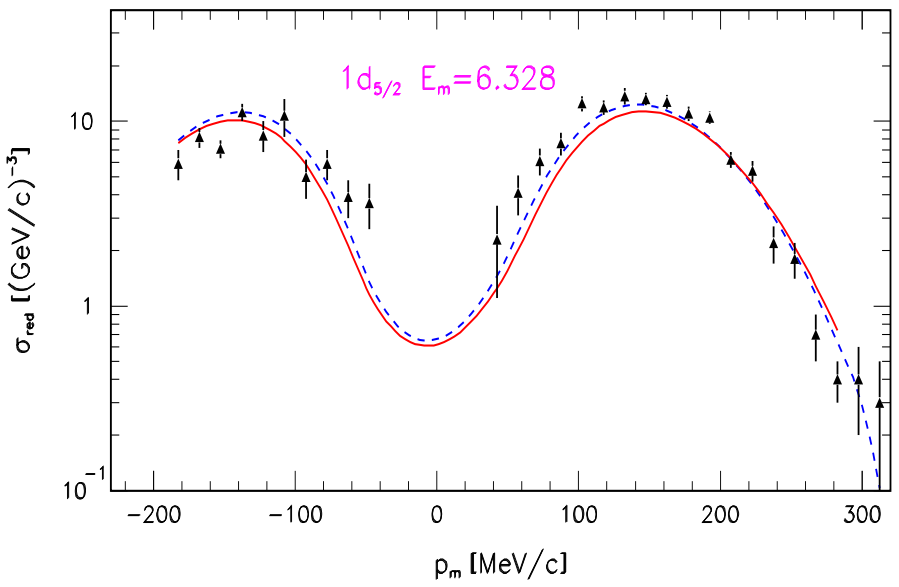

Comparison of the RDWIA calculations for electron reduced cross sections for the removal of nucleon from $\mathbf{2s_{1/2}}$ and $\mathbf{1d_{5/2}}$ shells of ^{40}Ca and ^{40}Ar as a function of missing momentum. The cross sections were calculated for NIKHEF [G.J.Kramer (1991)] kinematics: $\boldsymbol{\varepsilon_i = 483}$ MeV, and $\boldsymbol{T_x = 100}$ MeV. Negative values of $\boldsymbol{p_m}$ correspond to $\boldsymbol{\phi = \pi}$ and positive ones to $\boldsymbol{\phi = 0}$.

Inclusive cross sections

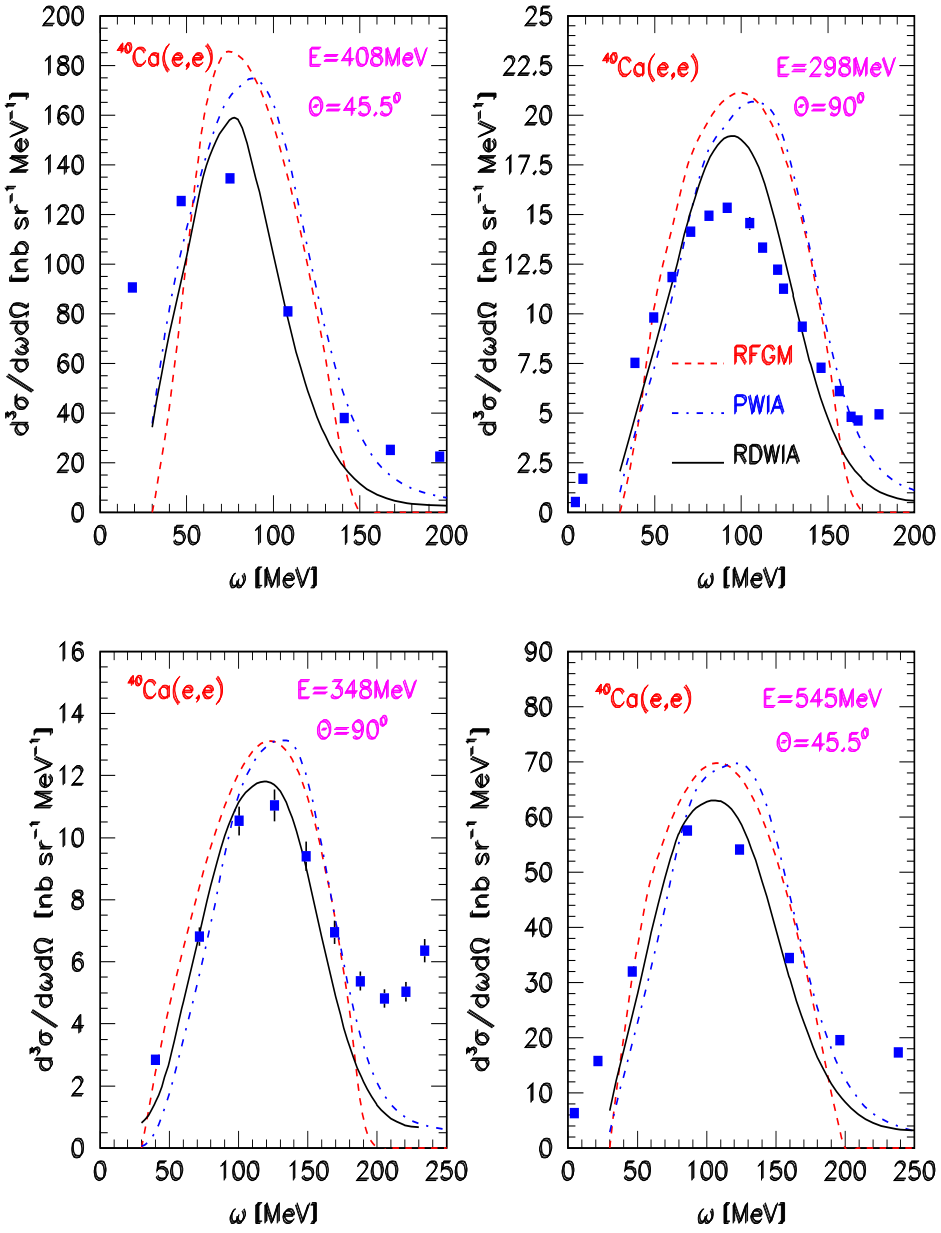

Inclusive cross section versus the energy transfer ω for electron scattering on ^{40}Ca. The data are from MIT Bates for electron beam energy E_e=408, 545 MeV and scattering angle θ=45.5° and for energy E_e=298, 348 MeV and θ=90°. The solid line is the RDWIA calculation while the dashed-dotted and dashed lines are respectively the PWIA and RFGM calculations.

Inclusive cross sections

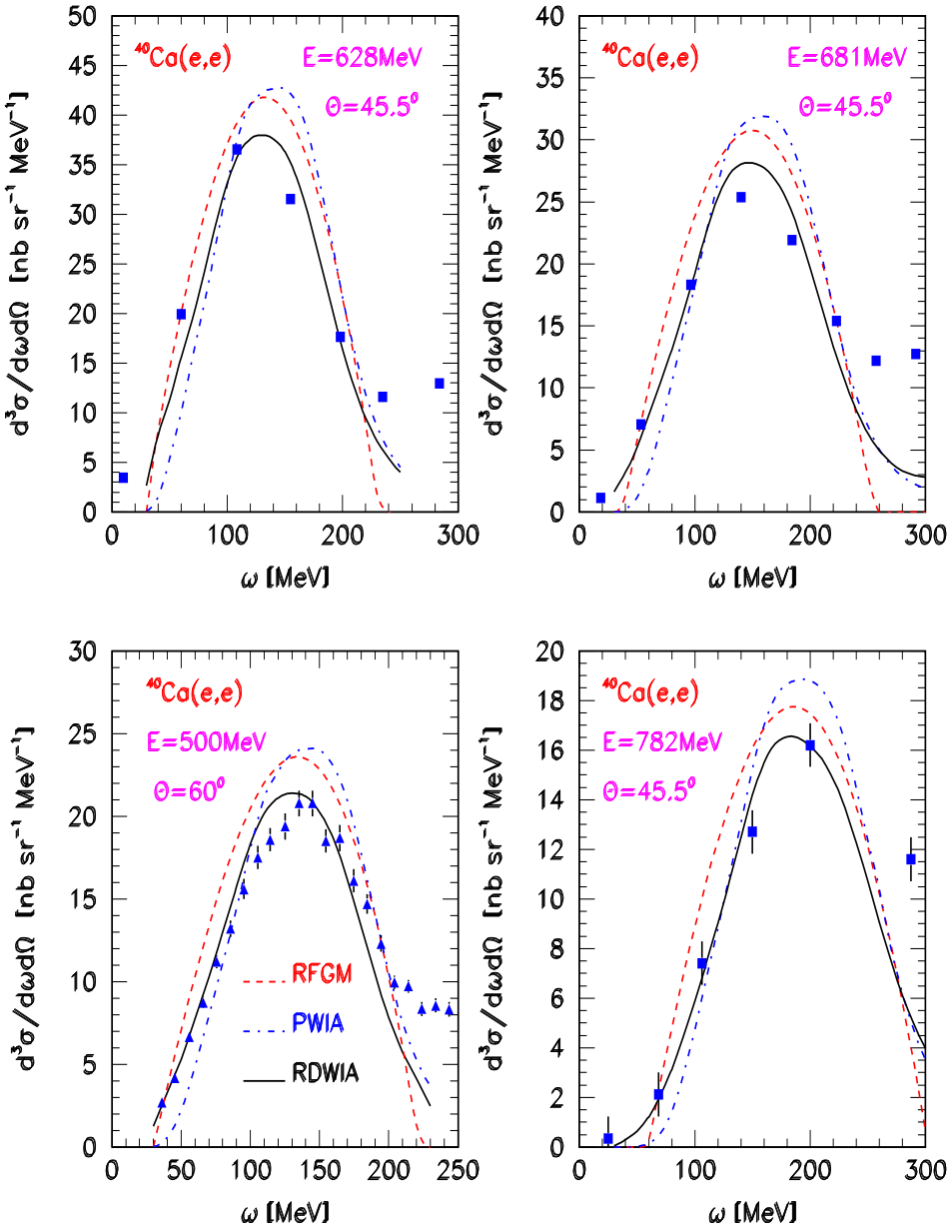

Inclusive cross section versus the energy transfer ω for electron scattering on ^{40}Ca. The data are from MIT Bates for electron beam energy E_e=628, 681, and 782 MeV and scattering angle θ=45.5° and from SLAC for energy E_e=500 MeV and θ=60°. The solid line is the RDWIA calculation while the dashed-dotted and dashed lines are respectively the PWIA and RFGM calculations.

Inclusive cross sections

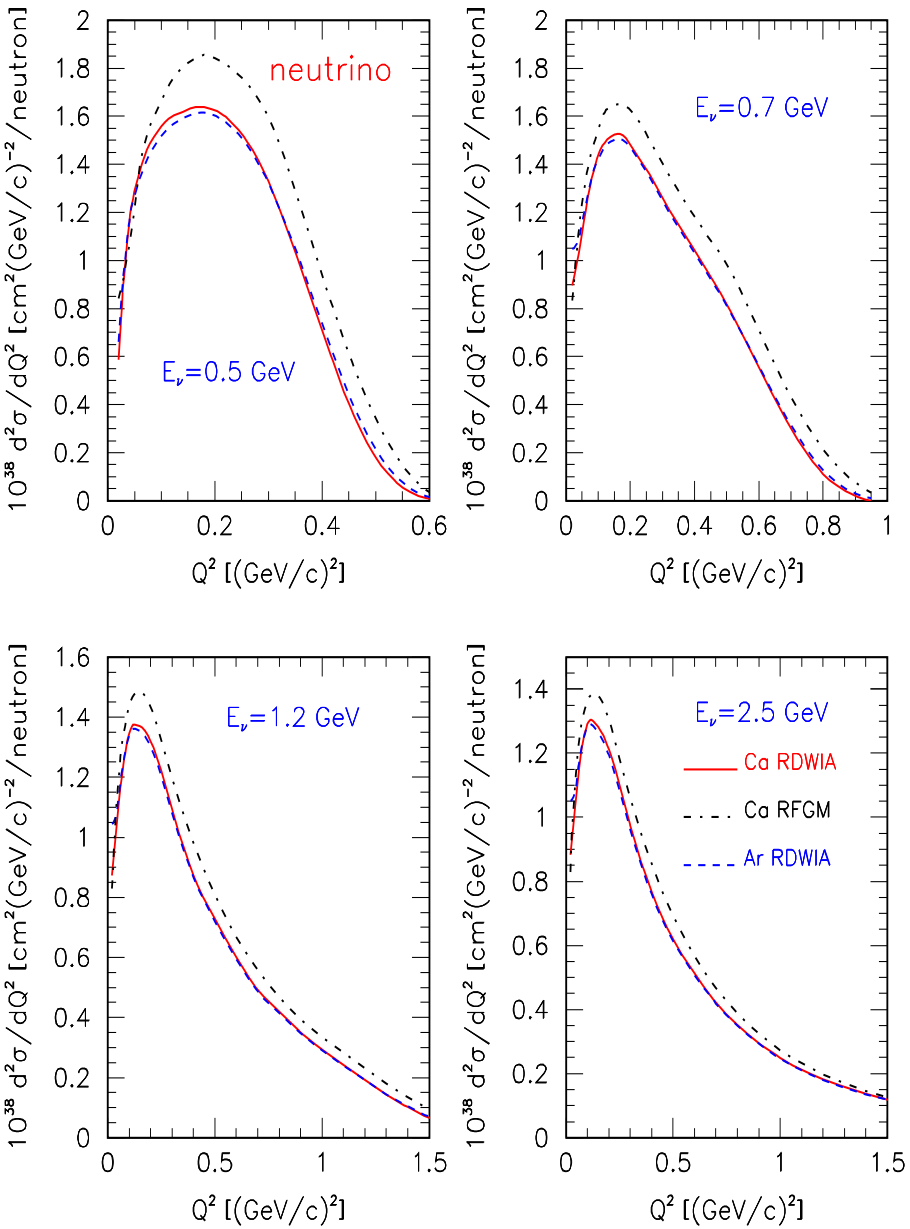

Inclusive cross section per neutron versus Q^2 for neutrino scattering on ^{40}Ca and ^{40}Ar and for four values of incoming neutrino energy:ε=0.5, 0.7, 1.2, and 2.5 GeV. The solid(dashed) line is the RDWIA calculation for ^{40}Ca (^{40}Ar) and dashed-dotted line is RFGM calculations for ^{40}Ca.

Inclusive cross sections

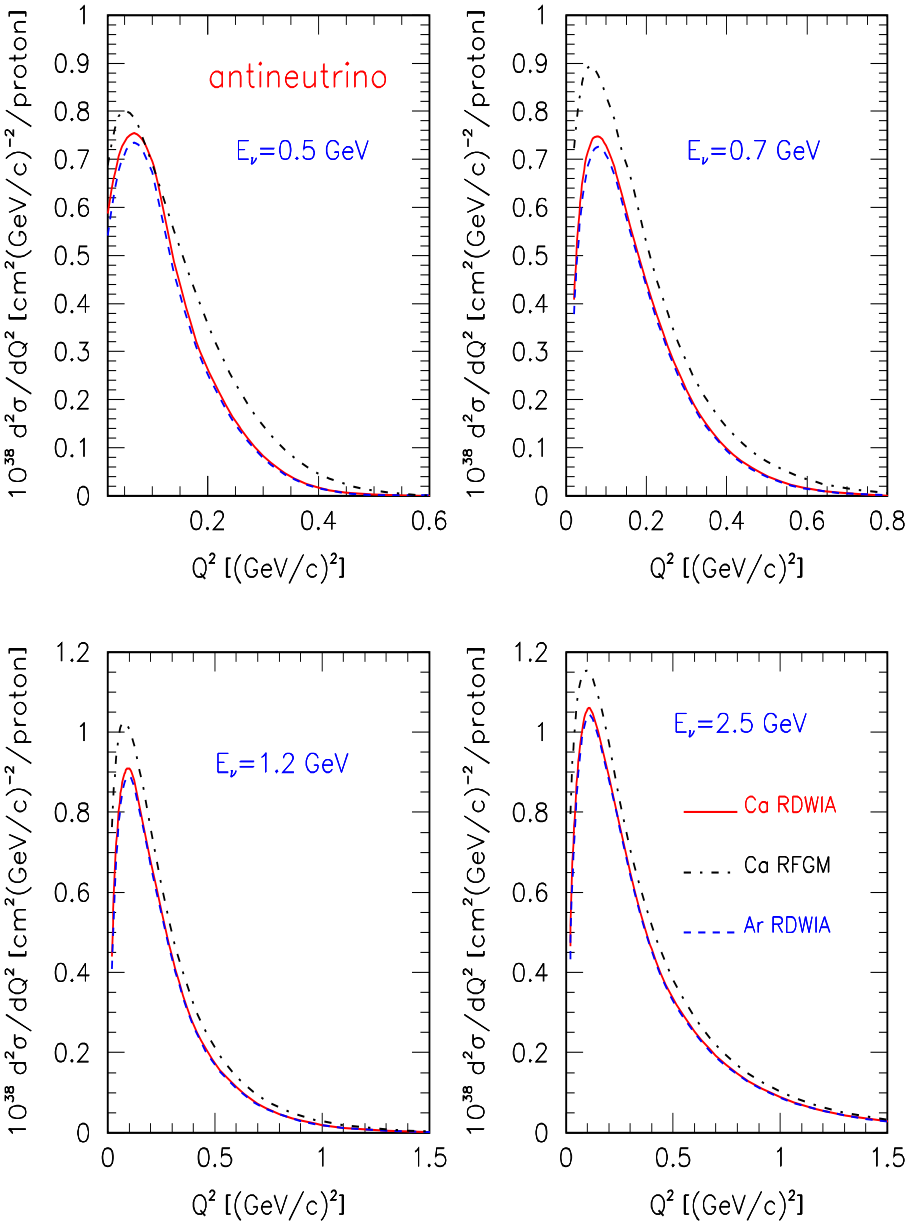

Inclusive cross section per proton versus Q^2 for antineutrino scattering on ^{40}Ca and ^{40}Ar and for four values of incoming neutrino energy:ε=0.5, 0.7, 1.2, and 2.5 GeV. The solid(dashed) line is the RDWIA calculation for ^{40}Ca (^{40}Ar) and dashed-dotted line is RFGM calculations for ^{40}Ca.

Total cross sections

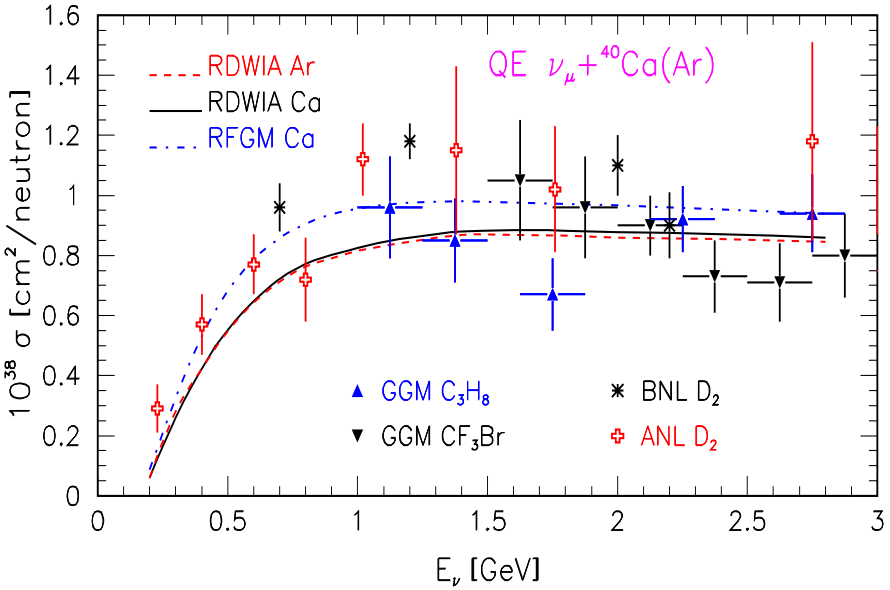

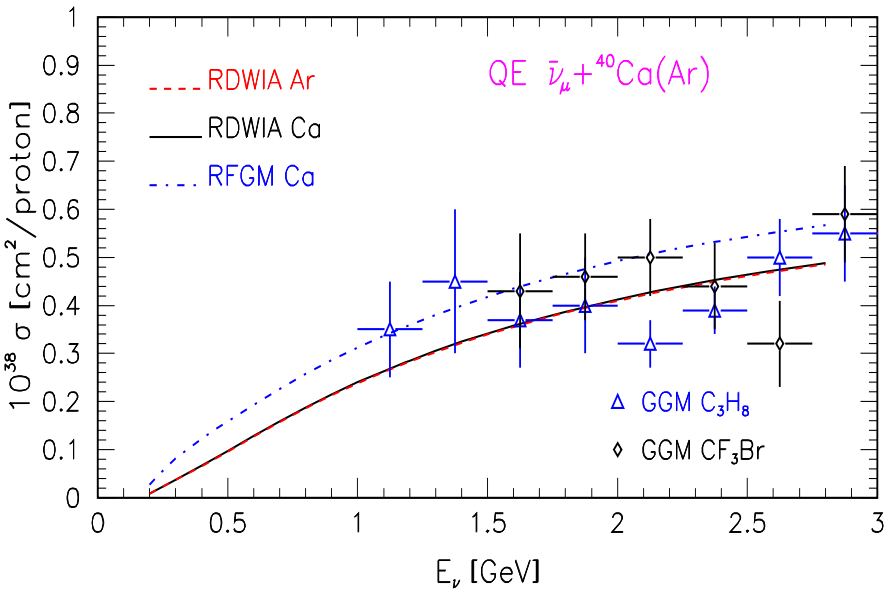

Total cross section for CCQE scattering of muon neutrino (per neutron, upper panel) and antineutrino (per proton, lower panel) on ^{40}Ca and ^{40}Ar as functions of incoming (anti)neutrino energy. The solid and dashed lines are respectively the RDWIA results for scattering on Calcium and Argon. The dashed-dotted line is the RFGM result for scattering on Calcium. These results were obtained with $M_A = 1.032$ GeV.

Total cross sections

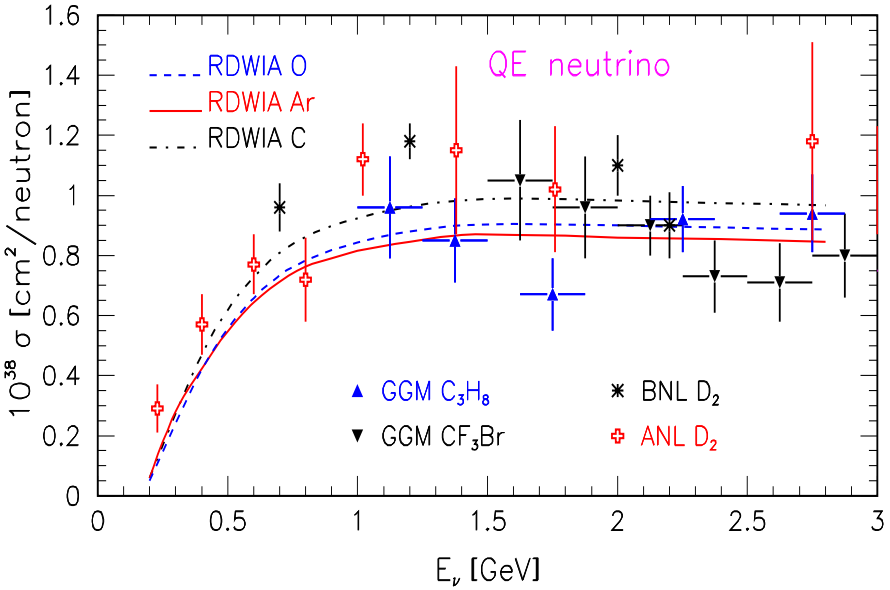

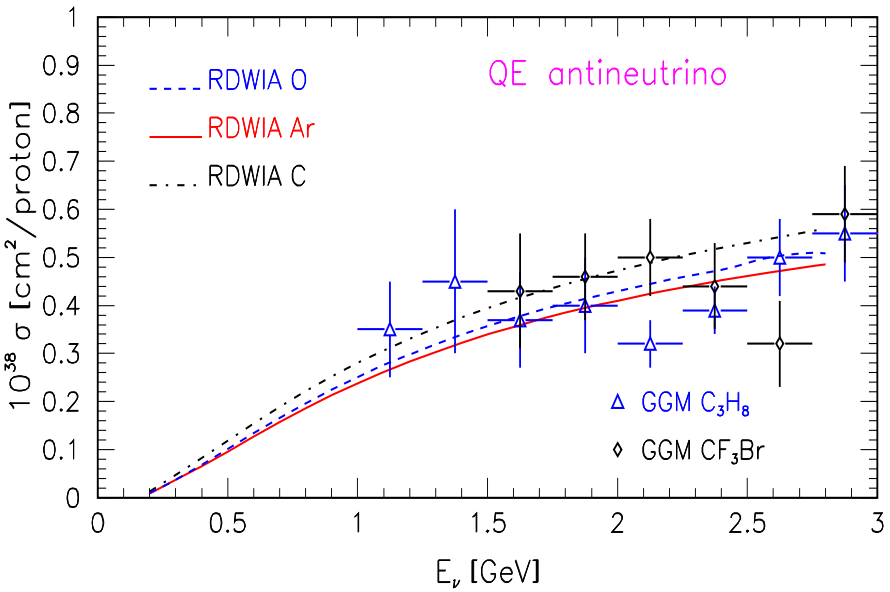

Total cross section for CCQE scattering of muon neutrino (per neutron, upper panel) and antineutrino (per proton, lower panel) on ^{40}Ar (solid line), ^{16}O (dashed line), and ^{12}C (dashed-dotted line) as functions of incoming (anti)neutrino energy. These results were obtained with $M_A = 1.032$ GeV.

DISCUSSION

Ratio O/C and Ar/C

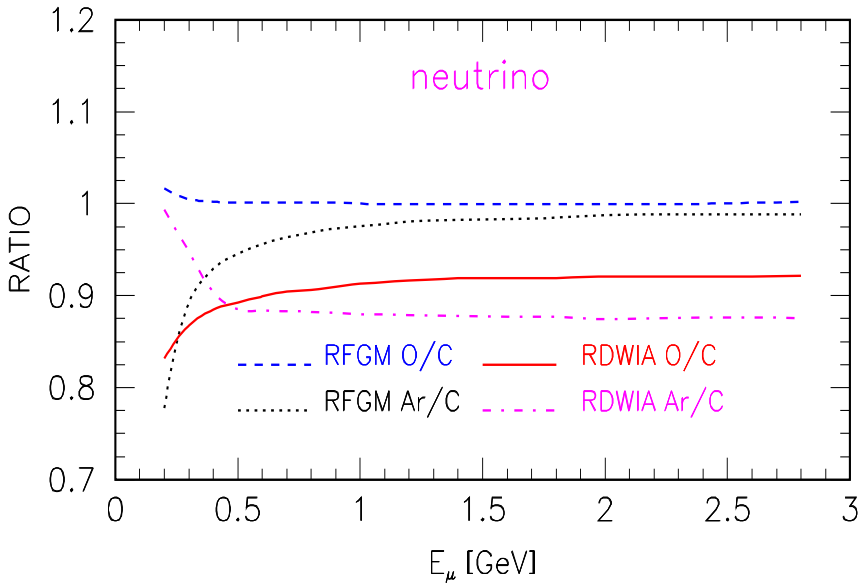

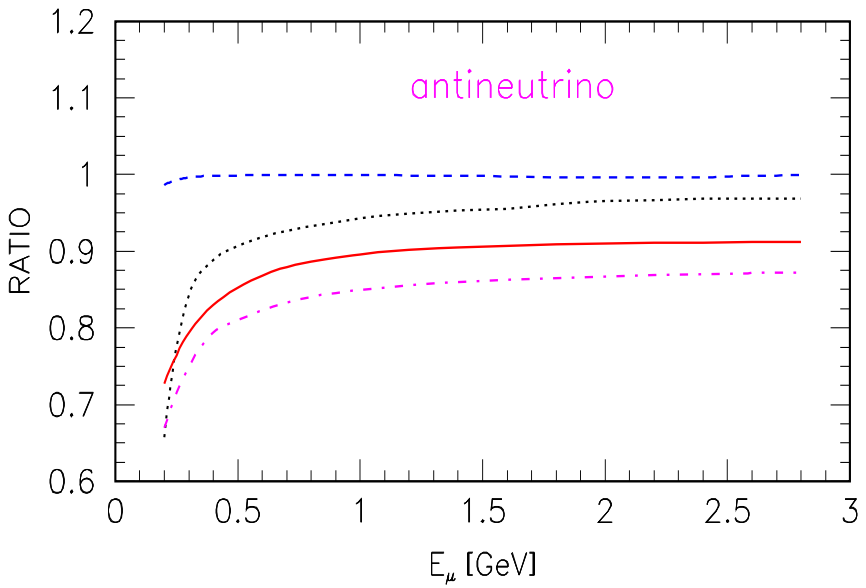

Ratio of the total cross section per neutron/proton R=O/C and R=Ar/C versus neutrino energy for neutrino (top panel) and antineutrino (bottom panel) scattering off ^{40}Ar, ^{16}O, and ^{12}C. The solid and dotted-dashed lines are the RDWIA results while dotted and dashed lines are the RFGM results, respectively.

Ratio Ar/C

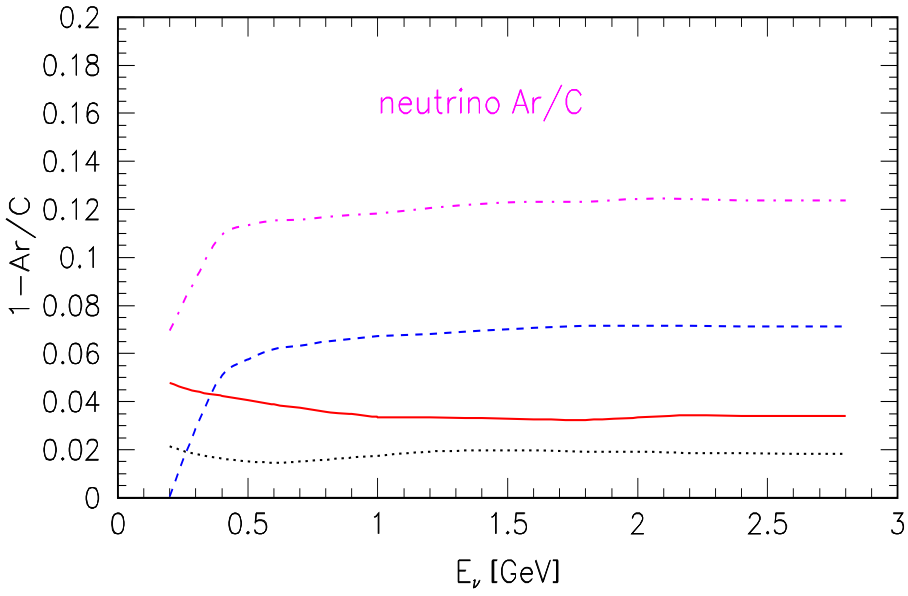

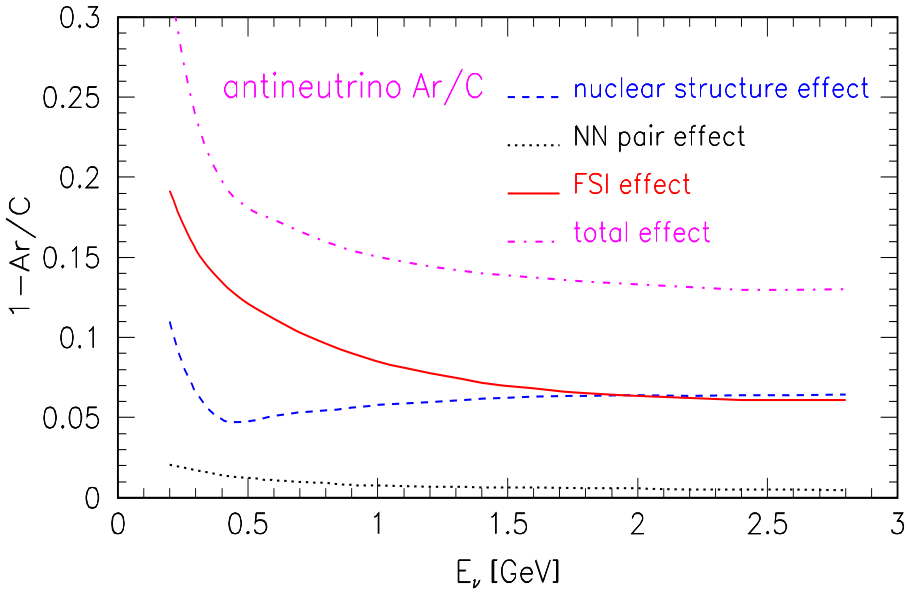

The difference between total cross section (per neutrino/proton) for neutrino (top panel) and antineutrino (bottom panel) scattering off ^{40}Ar and ^{12}C (1-Ar/C) due to different nuclear structures (dashed line), correlated NN-pair contributions (dotted line), and FSI effects (solid line). The dashed-dotted line is total of the three effects.

Ratio O/C

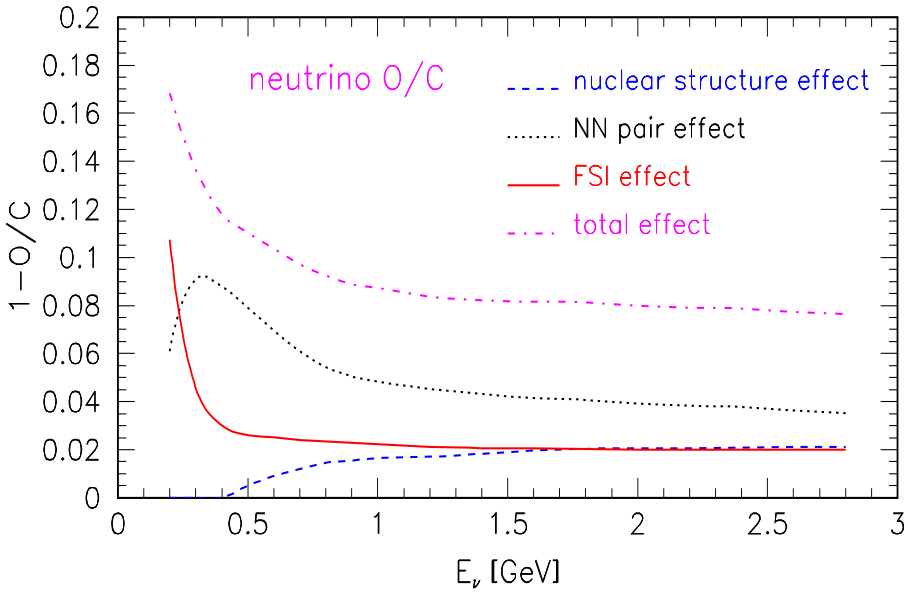

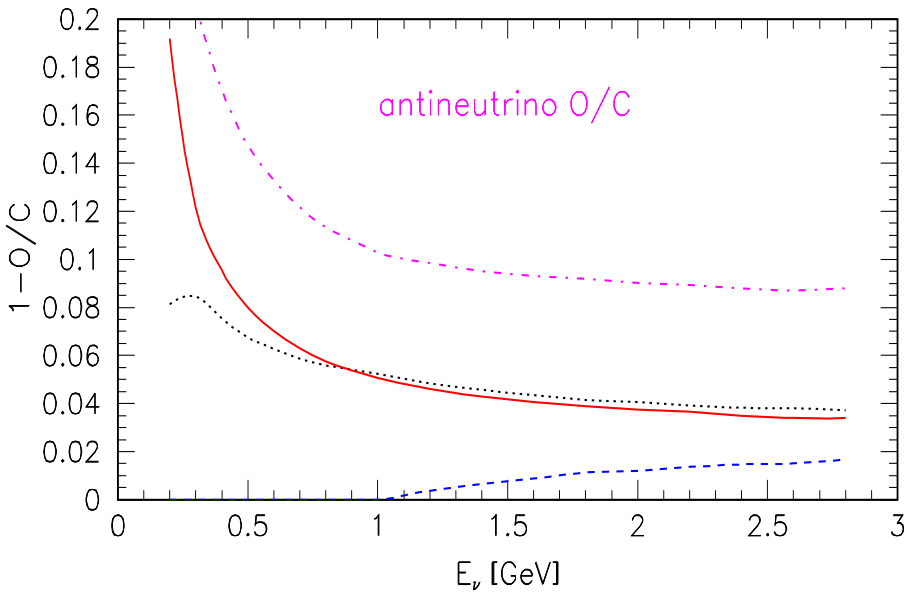

The difference between total cross section (per neutrino/proton) for neutrino (top panel) and antineutrino (bottom panel) scattering off ^{16}O and ^{12}C (1-O/C) due to different nuclear structures (dashed line), correlated NN-pair contributions (dotted line), and FSI effects (solid line). The dashed-dotted line is total of three effects.

Ratio O/C for electron scattering

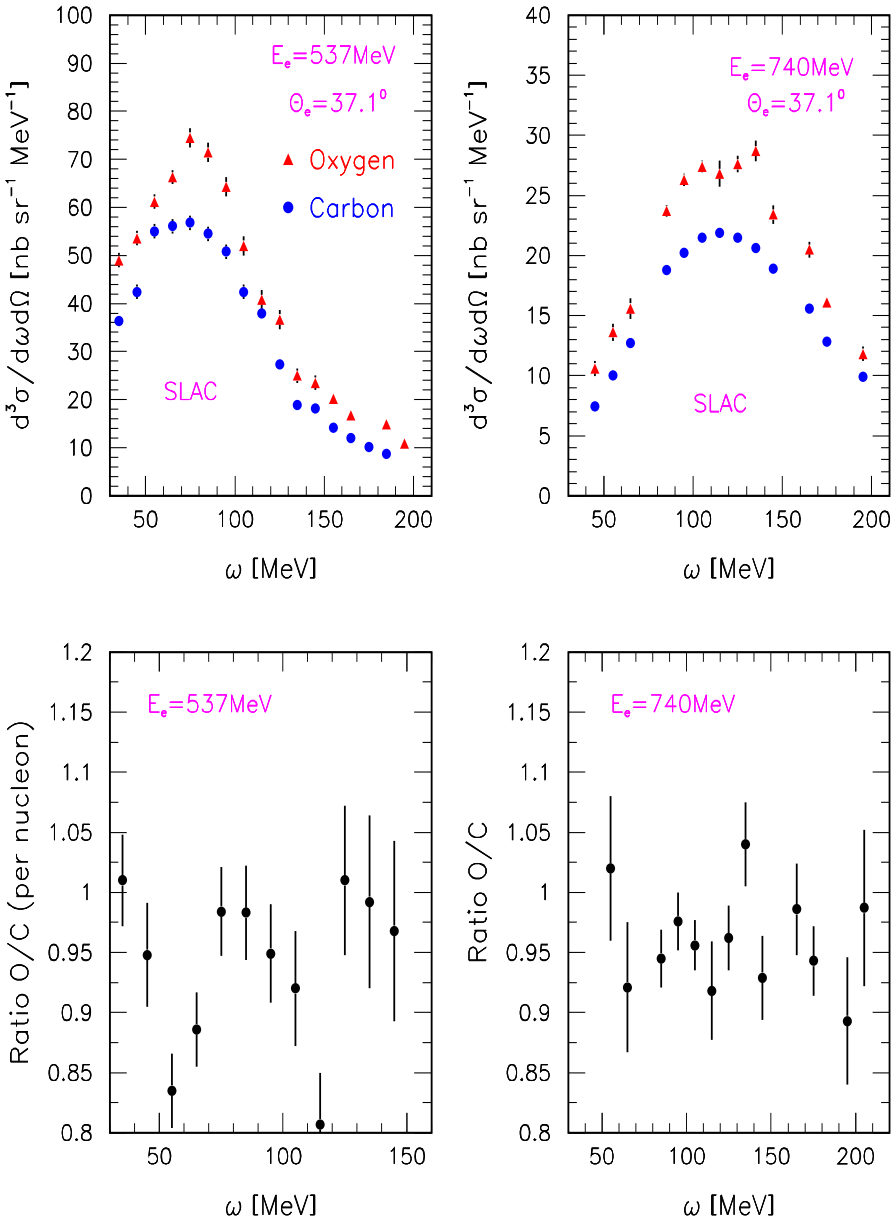

Inclusive cross section (top panel) and the ratio R=O/C per proton (bottom panel) versus energy transverse for electron scattering off ^{16}O and ^{12}C measured in SLAC experiment J.S. O'Connell et al. PRC 35,1063(1987) for electron beam energies $\boldsymbol{E_e = 537, 740}$ MeV and and $\boldsymbol{\theta}$=37.1°.

Ratio Ca/C for electron scattering

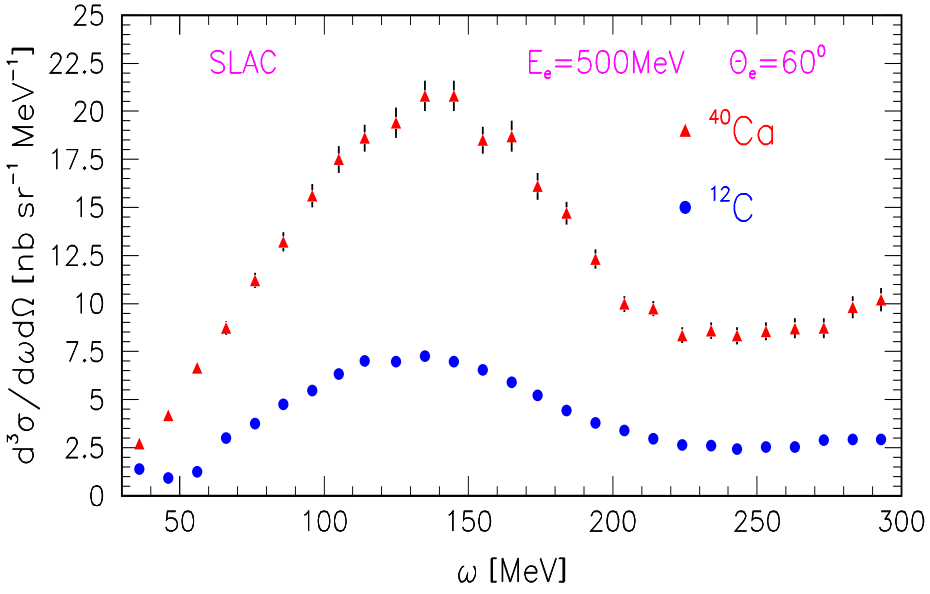

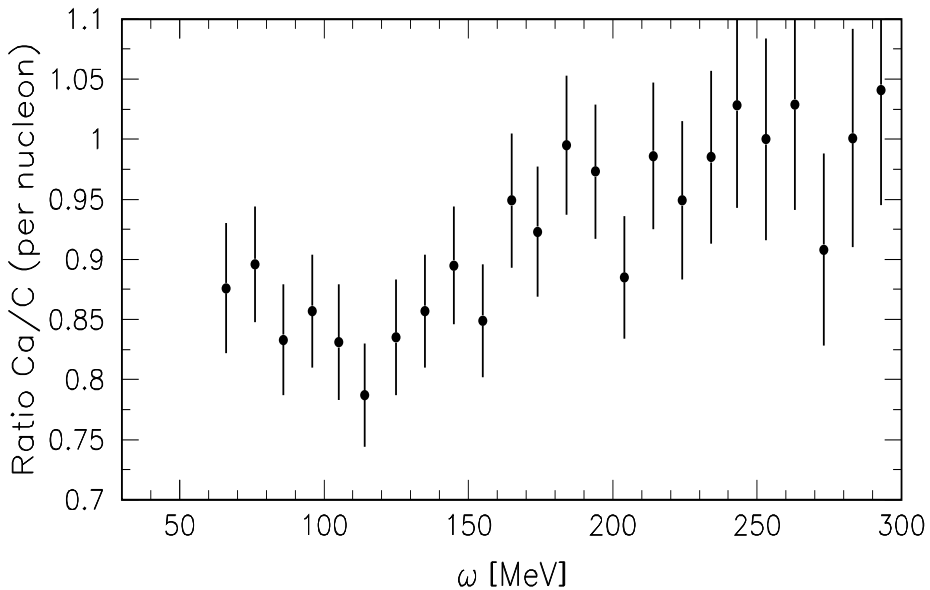

Inclusive cross section (top panel) and the ratio R=O/C per proton (bottom panel) versus energy transverse for electron scattering off ^{40}Ca and ^{12}C measured in SLAC experiment R.R. Whitney et al. PRC 9,2230(1974) for electron beam energy $E_e = 500$ MeV and and θ=60°.

CONCLUSIONS

Conclusions

QE CC $\nu(\bar{\nu})$ ^{40}Ca(Ar) cross sections were studied in different approaches.

- The reduced cross sections for neutrino and electron scattering off ^{40}Ca were tested against $^{40}Ca(e,e'p)$ data.
  - ⋆ In RDWIA the cross sections for $\nu(\bar{\nu})$ scattering are similar to those of electron scattering and in a good agreement with data (apart from small differences due to coulomb correction).

- The inclusive and cross sections were tested against ^{12}Ca(e,e') scattering data.
  - ⋆ In the peak region RFGM overestimates the value of inclusive cross section at low momentum transfer. The discrepancy with data decreases as momentum transfer increases.
  - ⋆ The RDWIA result is in agreement with data with accuracy 10-15%.

Conclusions

- The inclusive $d\sigma/dQ^2$ and total cross sections per neutron/proton for $\nu(\bar{\nu})^{40}$Ca(Ar) interaction were calculated in the RFGM and RDWIA approaches and compared with ones for (anti)neutrino scattering on Oxygen and Carbon.
  - ⋆ In the RFGM the cross sections per nucleon for Carbon are practically similar to those for Oxygen and Argon.
  - ⋆ In the RDWIA the cross sections for Oxygen and Argon are lower than those for Carbon and the difference is decreases as neutrino energy increases.
  - ⋆ The nuclear structure effects can be the main source of the difference between the total cross section (per neutron/proton) for (anti)neutrino scattering off off light and (medium)heavy nuclei.